



Published in final edited form as:

Ann Biomed Eng. 2017 January ; 45(1): 45–57. doi:10.1007/s10439-016-1668-5.

3D-Printing Technologies for Craniofacial Rehabilitation, Reconstruction, and Regeneration

Ethan L. Nyberg^{1,2,†}, Ashley L. Farris^{1,2,†}, Ben P. Hung^{1,2}, Miguel Dias^{1,2}, Juan R. Garcia³, Amir H. Dorafshar⁴, and Warren L. Grayson^{1,2,5,*}

¹Translational Tissue Engineering Center, Johns Hopkins University School of Medicine, Baltimore MD

²Department of Biomedical Engineering, Johns Hopkins University School of Medicine, Baltimore MD

³Department of Art as Applied to Medicine, Johns Hopkins University School of Medicine, Baltimore MD

⁴Department of Plastic and Reconstructive Surgery, Johns Hopkins University School of Medicine, Baltimore MD

⁵Department of Material Sciences & Engineering, Johns Hopkins University School of Engineering, Baltimore MD

Abstract

The treatment of craniofacial defects can present many challenges due to the variety of tissue-specific requirements and the complexity of anatomical structures in that region. 3D-printing technologies provide clinicians, engineers and scientists with the ability to create patient-specific solutions for craniofacial defects. Currently, there are 3 key strategies that utilize these technologies to restore both appearance and function to patients: rehabilitation, reconstruction and regeneration. In rehabilitation, 3D-printing can be used to create prostheses to replace or cover damaged tissues. Reconstruction, through plastic surgery, can also leverage 3D-printing technologies to create custom cutting guides, fixation devices, practice models and implanted medical devices to improve patient outcomes. Regeneration of tissue attempts to replace defects with biological materials. 3D-printing can be used to create either scaffolds or living, cellular constructs to signal tissue-forming cells to regenerate defect regions. By integrating these three approaches, 3D-printing technologies afford the opportunity to develop personalized treatment plans and design-driven manufacturing solutions to improve aesthetic and functional outcomes for patients with craniofacial defects.

* **Corresponding Author:** Warren L. Grayson, PhD, Johns Hopkins University, Department of Biomedical Engineering, Translational Tissue Engineering Center, 400 N. Broadway, Smith 5023, Baltimore, MD 21231, U.S.A. wgrayson@jhmi.edu.

† These authors contributed equally to this work.

Financial Relationships and Conflicts of Interest

The authors declare no conflict of interest.

No animal or human studies were carried out by the authors for this article.

Keywords

Facial prosthetics; craniofacial implants; tissue engineering; regenerative medicine; 3D-printing; scaffolds

1. Introduction

Craniofacial defects arise as a direct result of trauma, oncological resection, or congenital differences. They cause soft tissue or bone deficits, or a combination of both leading to non-healing composite tissue wounds. Defects in the craniofacial region in particular are difficult to treat because of the emphasis on positive aesthetic outcomes and the number of tissue types (bone, cartilage, muscle, and skin) and structures (auricle, orbit, nose, oral cavity) in close proximity. The current options for reconstructive surgery to treat these defects include grafts, local tissue rearrangement which fills defects with adjacent healthy tissue, microsurgical tissue transfer whereby one area of the body is transferred with its blood supply to another area^{10,22}, and vascularized composite allotransplantation whereby a portion of the body containing skin, muscle and/or bone is transplanted from one patient to another¹⁶. However, the major challenges with using traditional reconstructive surgery to treat large craniofacial defects are donor-site morbidity and procuring sufficient donor tissue with the same properties, including skin color, quantity and contour of bone, and quantity and quality of subcutaneous tissues, as the surrounding recipient tissue to restore normal anatomic structure and primary organ functions.

The challenge of integrating the various tissues of the face while maintaining or improving aesthetics motivates collaboration between the fields of prosthetic rehabilitation, craniofacial reconstruction, and regenerative medicine. **Prosthetic Rehabilitation** refers to the use of custom-made facial prosthetics to restore normal facial appearance (Figure 1A).

Reconstruction of the craniofacial region can be performed using a variety of plastic surgery techniques to replace structures and is aided by the precise manufacture of cutting guides, fixation devices, practice models and implanted medical devices (e.g. Figure 1B).

Regeneration aims to stimulate regrowth of damaged or malformed craniofacial tissues using stem cells and biologically active scaffold materials. (Figure 1C). For a particular defect, these approaches may be employed individually or in conjunction with one another. However, a common thread is the need for patient-specific treatments that fit a particular defect site to achieve both aesthetic cosmesis and functional replacement. As such, 3D-printing techniques that can create highly complex craniofacial geometries with high fidelity are well-suited for addressing particular needs.

Anatomical geometries can be captured using medical imaging such as computed tomography (CT), magnetic resonance imaging (MRI), or light scanning and then 3D-modeled digitally to create useful 3D-printed products. The particular method of 3D-printing affects the print outcome and may be selected based on the particular applications (Table 1). The primary methods for 3D-printing include fused deposition manufacturing (FDM), stereolithography (SLA), selective laser sintering (SLS), inkjet printing, inkjet bioprinting, extrusion bioprinting, and laser assisted bioprinting, which have been reviewed

extensively^{50,56}. Briefly, in FDM, molten material is extruded layer-by-layer onto a bed; once the material cools and solidifies, it serves as the foundation for the layer above it. While this method is easily applied to many materials – any material that can be melted and extruded – it requires support structures for printing overhangs. SLA uses a laser to solidify photocurable liquid polymers in a layer-by-layer fashion.⁵⁶ In contrast, SLS creates structures by sintering a powder bed layer-by-layer. The powder that is not sintered therefore serves as the support structure. A variation of this method, inkjet writing, also uses a powder bed, but uses a chemical binder instead of a laser to bind the particles together. The similarly named, inkjet bioprinting, uses acoustic, thermal, or electromagnetic forces to eject hydrogel droplets, which could contain cells or biological molecules, onto a platform in an additive fashion, onto a clean print bed or a binding solution.⁵⁶ Extrusion bioprinting is similar to inkjet printing, but uses pumps, screws, or pneumatic systems to extrude cell slurries with viscosities too high for inkjet printing. Finally, laser-assisted bioprinting consists of a laser source, a glass “ribbon” covered with a layer of cells in hydrogel solution, and a receiving substrate. The laser vaporizes a small portion of the hydrogel solution, which forms a bubble that can then fall as a droplet onto the platform below.⁵⁶

In this review, we examine how recent developments in 3D-printing enable more effective personalized treatment of complex craniofacial defects. We highlight advances in 3D-printing as applied to prosthetic rehabilitation, surgical reconstruction, and tissue regeneration for non-healing defects in the craniofacial region and identify avenues for further research.

2. 3D-printing for Prosthetic Rehabilitation

Recapitulation of patient specific coloring, texture, stiffness, and shape for prostheses is currently a labor-intensive process, which could be streamlined using 3D-printing. Prosthetic rehabilitation may be used in cases where successful surgical reconstruction is not a viable option due to factors such as poor prognosis, co-morbidities, compromised healing due to poor vascularization⁷⁹, and patient refusal of further surgical interventions². Further, the economic burden and treatment time for prosthetic rehabilitation is lower than that of surgical reconstruction⁷². Typical sites for craniofacial prosthetic rehabilitation include oral, orbital, nasal, and auricular regions^{51,71}. Prosthetic rehabilitation can also serve as an interim strategy during the period of treatment planning for a later surgical reconstruction⁶⁹. Besides providing an aesthetic solution to covering an affected area, prosthetic devices are considered medically necessary due to the functional benefits they offer to warm incoming air, maintain humidity of moisture filled cavities, protect fragile tissue, modulate speech, and provide support for corrective eyeglasses.

Treatment of craniofacial defects with prostheses traditionally involves the creation of a custom made device generally made of polydimethylsiloxane (PDMS) to replace missing tissue and cover underlying tissue^{51,71}. The workflow for creating these devices has gone relatively unchanged since the 1970's. However, the use of advanced 3D imaging techniques (including surface laser scanning and stereo photogrammetry) combined with 3D-printing is changing what was once a traditionally based workflow to include several facets achieved through digitally analogous methods (Figure 2). Only one study to date has reported a

clinically viable workflow for directly 3D-printing these devices³¹. It is still limited, however, as it does not result in a fully colored prosthesis with physical properties similar to the PDMS devices typically made by traditional methods. An alternate approach has been to 3D-print a negative multiple-piece mold that can be used for casting the final PDMS prosthesis. Advanced digital technologies and additive manufacturing techniques can thus be leveraged in craniofacial cases to increase the quality of outcomes for prosthetic rehabilitation. Future development of methods to directly print fully colored PDMS prosthetics could significantly improve manufacture time and costs for craniofacial prostheses. A number of companies are developing technologies to directly print PDMS^{80–82} and new techniques to precisely color complex and soft constructs (such computational hydrographic printing⁷⁷) offer exciting methods to fully recapitulate the appearance of the prosthetic.

3. 3D-printing for Surgical Reconstruction

3D modeling and manufacturing tools can provide aid in the personalized, surgical reconstruction of complex craniofacial defects by precisely cutting tissues according to preoperative plans, decreasing the total time and cost of surgery, and planning the shape of alloplastic and metal materials. Furthermore, such tools have helped to improve precise shaping and positioning of the newly incorporated tissues and improved the cosmetic and functional outcome of reconstructive operations⁴⁵ and are useful for patient education¹⁵. Tools that are used transiently in the reconstruction process, such as placement or cutting guides, are produced using FDM or SLA out of sterile and bioinert materials such as acrylonitrile butadiene styrene (ABS), poly(methylmethacrylate) (PMMA), or polypropylene⁵⁵. Implanted products additionally require long-term biocompatibility and mechanical strength and are often laser sintered from titanium or bioglass. Both types of products are often accurate to the millimeter scale.

3.1 VSP and Guides

Advances in 3D imaging and manipulation of the resulting datasets have enabled surgeons to plan surgeries using computer models of the patient, virtually moving bones and other tissue to assess different approaches, options, and outcomes (Figure 3). This virtual surgery planning, together with rapid physical modeling of the defects and custom cutting and positioning guides, has vastly improved preoperative planning techniques compared to more traditional approaches, and has significantly aided the surgeon in his or her approach to complex craniofacial reconstruction^{20,63}. 3D modeling and virtual planning aids intraoperative precision and efficiency of the surgery to match the preoperative design. Models of the defect site and the transferred bone segments can be manufactured to practice positioning, fixation, and evaluate aesthetic outcomes⁶⁶. Such planning segues easily into precise, custom cutting and placement guides, increasing cosmesis and reducing ischemia and total surgery time. Consider the clinical standard for reconstruction of mandibular bone, the free fibular flap⁵⁹: the fibula and the defect site are first scanned using CT (Figure 3A), then cuts are made in the fibula to adequately position the grafted bone into the defect site (Figure 3C). To aid in the precision of harvesting and repositioning the pieces of fibula, cutting and placement guides are designed and rapidly manufactured, often through FDM

(Figure 3D). Finally, custom surgical guides have been essential in enabling the advent of facial transplants—in addition to the planning and guide fabrication, 3D-printing is essential in preparing an exact fit for the donated face⁹.

3.2 Pre-fitting Implants

Rapid prototyped models of the defect, or the predicted defect, are also used to pre-bend generic off-the-shelf implants such as reconstruction plates and titanium meshes to fit the specific anatomy of the patient. Such precise and methodical pre-bending can result in improved functional and aesthetic outcomes⁶, decreased subjectivity²⁹, and reduced surgery and ischemia time⁶³. Stereolithographic models of the defect site have also been used to mold PMMA to fashion an alloplastic bone-graft alternative²¹. In addition, 3D-printing models of ideal and patient-specific anatomy produced by mirroring a normal contralateral side has been used to press fit a composite titanium and porous polyethylene implant, and then guide the surgical placement in order to reconstruct the orbital floor after facial trauma⁶¹. These methods allow for the customization of patient implants without significantly changing the manufacturing process of the device, which is a major regulatory and production hurdle.

3.3 Materials for Patient Specific Implants

Non-resorbable implants can be designed and manufactured specific to individual patients and can be used in lieu of autologous tissue⁵⁷. Many materials including metals, bioglasses, and bioinert plastics can be used in a number of manufacturing processes and maintain biocompatibility over time. For example polyetheretherketone (PEEK) has strong biocompatibility, mechanical strength, and radiographic translucency and can be 3D fabricated into patient specific implants through laser sintering or Computer Numerical Control (CNC) machining³⁹. In addition, patient-specific titanium mesh can be manufactured via direct metal laser sintering to hold grafted bone in place and re-create contours and structures of the facial bone⁶⁷. Bioglasses (such as S53P4, 6P53B, and 13–93) have been widely used in craniofacial surgery as a bone graft substitute due to their biocompatibility, strong mechanical strength, and osteoconductivity^{1,27}. Bioglass structures can be manufactured by mixing glass particles into a solution, cold-printing in a layer-by-layer fashion, and then dehydrating at high temperatures to sinter the glass particles together and remove the solution^{23,33}. Others have reported formulations of bioglass (such as 13–93 which has the composition 53SiO₂, 6Na₂O, 12K₂O, 5MgO, 20CaO, 4P₂O₅; wt.%) which can be laser sintered into anatomic shapes⁴³. Hydroxyapatite (the main component of bone) implants, via a resin carrier, can be produced through SLA and have been used to reconstruct large (>20 cm²) defects with resolutions less than 0.4mm⁸. Finally, in 2012 a titanium mandible was laser sintered and implanted into an 83-year-old patient. The patient was able to speak and swallow the same day, and exhibited excellent restoration of facial aesthetics²⁸. While titanium is the industry standard in orthopedic implants, the cost of materials, unknown long term efficacy, and manufacturing remain limiting. There is particular concern of implant exposure and infection over time as there is often only a thin layer of soft tissue covering the implant.

As the intersection of 3D imaging, manipulation, design, and manufacturing develops further, these tools for surgeons will broaden from individual case studies to common practice. The past decade of developing these tools apace with the maturation of 3D technology will likely revolutionize surgical standards, just as 3D-printing has revolutionized transradial prostheses^{17,83}. Increased efficiency and accuracy provided by these tools will be driving factors of their widespread adoption while regulatory, biocompatibility, and reimbursement challenges remain⁴. Innovation stimulated and facilitated by these 3D technologies will also continue, leading to techniques as impressive as the recent total face and jaw transplants^{9,16}.

4. 3D Printing for Craniofacial Bone Regeneration

The goal of a 3D-printed construct for regeneration is to fill the defect with biological tissue. To accomplish this, an appropriately shaped construct can be produced that is populated uniformly with tissue-forming cells that are signaled to regenerate tissue. This can be accomplished in two ways: printing of acellular scaffolds that can be populated with cells prior to implantation or the printing of living, cellular constructs, termed ‘*bioprinting*’.

4.1 Acellular printing

Several key parameters should be considered and optimized for scaffold development: (1) macro-geometry (Figure 1C), (2) micro-architecture, (3) bioactivity, and (4) mechanical properties (Figure 4). The strengths and weaknesses of these currently investigated printing approaches to achieving the four considerations outlined above are discussed below.

Incorporating micro-architecture, which encompasses pore geometry and pore size, is critical for uniform cell distribution and cell migration into the scaffold; interconnected pores can improve integration of regenerated tissue with native tissue.⁴⁶ For bone tissue engineering *in vivo*, higher porosity has been correlated with increased bone ingrowth into scaffolds.³⁶ Designing pore architecture results in higher pore connectivity and uniform cell distribution compared to random architecture resulting from salt-leaching methods, despite similar porosity, pore size, and surface area⁵². Pore size and interconnectivity also improves nutrient diffusion into and waste diffusion out of scaffolds.⁶⁰ Scaffold vascularization, a critical component of tissue survival, has been shown to increase with increasing pore size; pore sizes between 160–270 μm resulted in extensive vessel formation in both mathematical and experimental models^{3,13}. Osteoblast proliferation and migration through collagen-glycosaminoglycan scaffolds also depends on pore size, with larger pores around 300 μm resulting in higher cell numbers throughout the scaffold⁵⁴. In the context of 3D-printing, some methods are better suited to creating defined pores. For instance, FDM relies on rapid cooling of an extruded molten material, resulting in well-defined scaffold struts and well-defined pores⁷⁰. In contrast, chemical binding-based approaches rely on dispensing a liquid binder onto a powder substrate and result in pore sizes less than 100 μm due to binder flow³⁸.

The scaffold should also provide biological signals to resident cells to form tissue. For bone, the most widely used strategy is incorporation of mineral phases in scaffolds for osteoinductivity⁵; similar strategies have been investigated with 3D-printed scaffolds. For

example, a phosphoric acid binder was used to bind calcium phosphate together, creating a mineralized structure that can house cells³⁸. Another method used polycaprolactone (PCL) with incorporated tricalcium phosphate particles in FDM⁶⁵. In addition, incorporation of bioactive molecules, such as bone morphogenetic proteins (BMPs), have been investigated; however, given most 3D-printing methods rely on high temperatures, up to 1300 °C for sintering methods⁶⁸, use of growth factors in 3D-printing remains a challenge. Chemical binding methods have the distinct advantage of printing at room temperature, creating potential for application of the method to growth factor incorporation, though careful choice of binder is required to prevent pH-related damage. A second approach is to load growth factors onto a scaffold post-printing, which circumvents these issues but adds another step to scaffold manufacturing.

Finally, in the replacement of craniofacial bone, the scaffold must provide structural support for both resident cells and for transduction of mechanical forces through the craniofacial skeleton. Target scaffold stiffness depends on anatomical location, with the elastic modulus of human trabecular bone within the mandibular condyle ranging between 120–450 MPa or within the mandible from midline to ramus ranging from 112–910 MPa.³² Many current 3D-printed scaffolds have achieved stiffness within the 10–100 MPa range^{32,37,38,78}. Testing mechanical properties of polymeric scaffolds under physiological conditions is crucial as groups have shown changes in compressive moduli at different temperatures and in aqueous media.³⁷ It should be noted that increased porosity leads to lower mechanical properties – a study using sintered PCL reported that the stiffness of printed porous scaffolds was around 15 MPa, compared to 300 MPa for a solid PCL piece¹⁸. As such, the importance of porosity for cellular ingrowth and proliferation must be balanced against the importance of structural scaffold properties for mechanical support and force transduction.

The importance of these four criteria is clearly demonstrated in the clinical regeneration of soft and osseous tissue holding the left mandibular cuspid in place⁶². Using the patient's CT scan the exact macroscopic geometry of the scaffold was determined. The scaffold was printed using SLS of PCL containing 4% hydroxyapatite for osteoinductivity. In addition, the scaffold was designed to release platelet-derived growth factor BB (PDGF-BB), a factor known to support vascularization and mineralization^{30,34}, in a burst manner from pre-formed channels. Due to the high printing temperatures associated with sintering, the scaffold was first printed without growth factor and immersed in PDGF-BB solution for 15 minutes after printing. The use of PCL as the main biomaterial was justified from a mechanics standpoint: the stiffness of PCL scaffolds manufactured using SLS has been reported to be ~15 to 300 MPa, depending on porosity¹⁸, values that fall within the reported range for human trabecular bone.

The scaffold porosity or micro-architecture was not reported, though the lack of interconnected pores was noted as a limitation of the approach. The implantation of the scaffold was successful – the image-based geometry fit the defect well – and the printed channels for growth factor release successfully dispensed PDGF-BB in a burst manner.⁶² As a shortcoming, the patient presented with scaffold exposure and wound failure past 13 months post-implantation. Upon removal of the scaffold, histological analysis indicated a preponderance of connective tissue formation and little bone regeneration, suggesting the

lack of internal micro-architecture prevented the infiltration of regenerative and vascular cells and therefore precluded regeneration. Combined with the slow-degrading properties of PCL, the authors concluded that the scaffold's low porosity served to block tissue regeneration. As such, while the macro-geometry and mechanical properties were appropriate (over the 13-month period, the scaffold did not fail mechanically despite being in a region of load), the lack of micro-architecture inhibited the bioactive and regenerative properties of the scaffold.

This example of the clinical application of 3D-printing scaffolds for craniofacial regeneration highlights strengths and necessary improvements. The combination of image-based extraction of craniofacial geometry and the ability to 3D-print shapes with high fidelity resulted in a scaffold tailored to the specific defect. The ability to incorporate bioactive factors into the printed scaffold was also demonstrated. Finally, the choice of PCL as a printable biomaterial illustrated the ability to print mechanically appropriate scaffolds for load-bearing craniofacial regions. In addition to the group featured in this case study, other groups have commercialized FDA-approved PCL scaffolds fabricated by FDM.⁸⁴

A relatively underexplored area of 3D-printed scaffolds involves printing biological and mechanical gradients. For example, printing scaffolds with hydroxyapatite gradients could improve bone formation with exterior areas having more mineral to encourage growth of compact bone and interior areas having more diffuse mineral to mimic trabecular bone. While printing with growth factors has been a challenge due to printing conditions for many techniques surpassing biological pH and temperatures at which these molecules are stable, several groups have printed bioactive ceramics or extracellular matrix (ECM)^{35,47}. The incorporation of ECM enhanced scaffold bioactivity, but high ECM concentrations decreased scaffold mechanics. Printing extracellular matrix proteins in 3D spatial gradients has been achieved by using maskbased SLA to stimulate assembly of genetically engineered photoactive proteins, though this was used as a surface modification for tissue culture rather than an implantable 3D construct⁷³. Another group used inkjet printing to create gradients of laminin and used their materials to study cell alignment¹¹.

Printing mechanical gradients by varying pore structure and size could also assist with building tissue that mimics native function, particularly in the bone example. One group has recently demonstrated that gradient pore sizes created by FDM can slightly improve both chondrogenesis⁴⁹ and osteogenesis⁴⁸, although they did not investigate different geometries. By designing scaffold pore sizes and geometries based on biological mechanical requirements, these improvements may be further enhanced.

4.2 Bioprinting

Bioprinting differs from the traditional tissue engineering approach of seeding cells onto preformed scaffolds by depositing cell and scaffold simultaneously, forming a predesigned structure²⁴. Bioprinting is the computer-aided deposition of living cells into 3D patterns. It is currently performed with micron-scaled precision⁵⁰. As cell viability must be maintained during the printing process, the methods used for bioprinting differ from those used for traditional 3D-printing. Important parameters of 3D-bioprinting scaffolds include (1) cell positioning, (2) bioink selection, and (3) mechanical strength. In many cases, the type of

bioink used and the required resolution dictates the optimal printing technique for a particular application.

Bioprinting offers a key advantage over the traditional approach of seeding cells into 3D-printed scaffolds: digitally designing layer-by-layer deposition of cells to precisely regulate 3D cell distribution. This is advantageous when designing vascularized soft tissue, as adequate nutrient and oxygen supplies are necessary during tissue regeneration.⁴² For example, Kolesky et al. developed a bioprinter that could print up to four cell types simultaneously and created complex 3D patterns of fluorescently labeled human dermal fibroblasts and human umbilical vein endothelial cells⁴⁴. However, there are also several challenges associated with cellular printing.

Another disadvantage of bioprinting compared to acellular printing is that the mechanical strength of bioinks is typically lower than thermoplastic polymers. Originally, the majority of bioinks were natural hydrogel polymers, particularly alginate and fibrin, which when printed have compressive moduli of approximately 5 kPa¹². Human bone and cartilage typically have moduli of about 10–20 GPa and 700 kPa, respectively²⁵. In order to print tissues having similar load-bearing capacities to native bone and cartilage, PEG-based hydrogels have been printed with compressive moduli between 300–350 kPa²⁶. Another method used to improve mechanical strength is integrating acellular and cellular bioprinting. Merceron et al. used a combination of FDM and extrusion bioprinting to print two thermoplastic polymers along with C2C12 and NIH/3T3 cells to create a 3D-printed muscle-tendon unit⁵³ and Kang et al. integrated FDM and extrusion bioprinting to print vascularized bone, muscle, and cartilage⁴⁰. Printing hybrid scaffolds with cellular and acellular components may be one way to improve mechanical strength of bioprinted scaffolds. These limitations are some of the reasons that bioprinting has not yet been used to regenerate craniofacial tissues in human patients.

Of the tissues necessary for craniofacial reconstruction, skin bioprinting is the nearest towards clinical translation, with studies conducted *in vivo* using mice and pigs. One study of note compared bioprinted scaffolds to a commercially available engineered skin graft (Apligraf)⁷⁵. A current limitation of engineered skin grafts such as Apligraf is that they lack microvasculature to maintain cell viability over time and instead rely upon diffusion to transport oxygen and nutrients to cells. Bioprinting can overcome this limitation by precisely patterning microvascular structures for skin grafts. Bioprinted scaffolds were trilayered with the top layer composed of collagen and printed keratinocytes, the middle layer composed of fibrin and endothelial cells, and the bottom composed of collagen and fibroblasts. Apligraf is a bilayered material cast with two collagen layers: one containing dermal fibroblasts and the other containing keratinocytes⁷⁴. The group found that wound contraction, which if excessive can be a marker for joint contraction, malfunction, and poor aesthetic outcomes decreased in the bioprinted scaffolds compared to Apligraf and no treatment, which were statistically similar. Additionally, the mice with printed grafts healed between 14–16 days, whereas those with no grafts or with Apligraf healed within 21 and over 28 days, respectively. Histologically, the printed groups showed microvessel formation by implanted human endothelial cells in the printed scaffolds. Macroscopic images of skin regeneration in Apligraf and bioprinted groups can be seen in Figure 5A–F. Patterning endothelial cells to

form lumenized microvessels to improve graft viability could allow for scale up in terms of graft thickness and area by reducing oxygen and nutrient diffusion limitations. Binder *et al* have developed a promising *in situ* bioprinter for skin, but initial preclinical tests in pigs demonstrated unsatisfactory healing outcomes in wound closure rates, which the authors suggested was due to an insufficient cell density (2.0×10^5 cells/cm²).⁷ While the bioprinted materials have improved skin wound healing in terms of decreasing wound contraction and healing time *in vivo* is a promising advance for skin bioprinting, but such methods are still inferior or comparable to cell spraying techniques⁷.

Bioprinting of bone has also moved forward, with some preliminary bioprinting studies conducted *in vivo*. Of particular import is a pilot study conducted by Keriquel *et al.* that investigated the use of laser assisted bioprinting to manufacture hydroxyapatite scaffolds directly into a calvarial defects in mice, as seen in Figure 5G, H⁴¹. When bone formation was measured by X-ray micro-tomography at the group observed considerable variation in bone formation between individual mice and did not provide quantitative data for bone ingrowth. Though these results are preliminary, they do show that bioprinting *in vivo* is possible and may have potential for clinical use with the proper bioink and cell source.

The precise patterning of biological molecules and cells through bioprinting may be useful in creating tissues with complex spatial orientations. Though the field is young, promising results have been achieved for skin and bone engineering *in vivo*. Studies have investigated cartilage¹⁴, muscle⁵³, and adipose⁵⁸ tissue engineering using bioprinting, though these have not yet advanced to *in vivo* studies. The expensive specialized equipment necessary to use bioprinting technologies and the added regulatory burden of incorporating cells into a biomaterial, acellular printing may be the preferred regenerative method for treating craniofacial defects. Bioprinting could be further improved by widening the selection of available bioinks, decreasing print time, increasing print resolution, and moving more studies towards *in vivo* models.

5. Conclusion

Craniofacial deformities, when they arise, are particularly debilitating as they impact emotional, psychosocial, and functional well-being of the affected individual. They are difficult to treat due to the geometrical requirements and multiplicity of tissue types that are impacted. However, recent advances in 3D-printing technologies hold tremendous promise for advancing treatment options available to patients. The requirements of 3D-printed products differ depending on the size and severity of the defects, which together with patient-specific factors determine whether the primary treatment modality is prosthetic rehabilitation, surgical reconstruction, or regeneration. For rehabilitation, the use of 3D-printing technologies to either directly create PDMS prosthetics or print molds has the potential to significantly streamline the associated workflows for this process. The prostheses are flexible, non-degradable, and need to incorporate patient-specific skin tones. They differ considerably from 3D-printed guides or alloplastic implants used in reconstructive surgeries. Perhaps the most transformative applications, of 3D-printing lie in the realm of tissue regeneration. This area remains relatively nascent to date and significant research efforts are being dedicated to its continue rapid advancements that include the

development of biodegradable scaffolds as well as bioinks used for printing live cells. The successful implementation of these technologies clinically will expand the treatment options available to patients.

Acknowledgments

This work was supported by an NIH Biomedical Engineering Training Grant (ELN), an NSF graduate research fellowship (ALF), an NIH pre-doctoral fellowship (BPH), and grants from the Maryland Stem Cell Research Fund and the Department of Defense (WLG).

Abbreviations

3D	Three Dimensional
ABS	Acrylonitrile Butadiene Styrene
BMPs	Bone Morphogenetic proteins
CNC	Computer Numerical Control
CT	Computed Tomography
ECM	Extracellular Matrix
FDM	Fused Deposition Modeling
MRI	Magnetic Resonance Imaging
PCL	Polycaprolactone
PDMS	Polydimethylsiloxane
PDGF-BB	Platelet-Derived Growth Factor BB
PEEK	Polyetheretherketone
PMMA	Polymethyl Methacrylate
PLA	Poly lactide
SLA	Stereolithography
SLS	Selective Laser Sintering
VSP	Virtual Surgery Planning

References

1. Aitasalo KMJ, Piitulainen JM, Rekola J, Vallittu PK. Craniofacial bone reconstruction with bioactive fiber-reinforced composite implant. *Head Neck*. 2014; 36:722–728. [PubMed: 23616383]
2. Ariani N, Visser A, van Oort RP, Kusdhany L, Rahardjo TB, Krom BP, van der Mei HC, Vissink A. Current state of craniofacial prosthetic rehabilitation. *Int. J. Prosthodont*. 2012; 26:57–67.
3. Artel A, Mehdizadeh H, Chiu Y-C, Brey EM, Cinar A. An agent-based model for the investigation of neovascularization within porous scaffolds. *Tissue Eng. Part A*. 2011; 17:2133–2141. [PubMed: 21513462]

4. Khanna, Ashok; Balaji, Sukhdev; Jawahar, Thanga; D, A. 3D Printing: New Opportunities for the Medical Devices Industry. 2015
5. Azami M, Samadikuchaksaraei A, Ali Poursamar S. Synthesis and characterization of a laminated hydroxyapatite/gelatin nanocomposite scaffold with controlled pore structure for bone tissue engineering. *Int. J. Artif. Organs.* 2010; 33:86. [PubMed: 20306435]
6. Azuma M, Yanagawa T, Ishibashi-Kanno N, Uchida F, Ito T, Yamagata K, Hasegawa S, Sasaki K, Adachi K, Tabuchi K, Sekido M, Bukawa H. Mandibular reconstruction using plates prebent to fit rapid prototyping 3-dimensional printing models ameliorates contour deformity. *Head Face Med.* 2014; 10:45. [PubMed: 25338640]
7. Binder, K. (Doctoral Dissertation). 2011. In situ bioprinting of the skin. Retrieved from Z. Smith Reynolds Library <http://hdl.handle.net/10339/33425>
8. Brie J, Chartier T, Chaput C, Delage C, Pradeau B, Caire F, Boncoeur MP, Moreau JJ. A new custom made bioceramic implant for the repair of large and complex craniofacial bone defects. *J. Cranio-Maxillofacial Surg.* 2013; 41:403–407.
9. Brown EN, Dorafshar AH, Bojovic B, Christy MR, Borsuk DE, Kelley TN, Shaffer CK, Rodriguez ED. Total face, double jaw, and tongue transplant simulation: a cadaveric study using computer-assisted techniques. *Plast. Reconstr. Surg.* 2012; 130:815–823. [PubMed: 22691839]
10. Broyles JM, Abt NB, Shridharani SM, Bojovic B, Rodriguez ED, Dorafshar AH. The Fusion of Craniofacial Reconstruction and Microsurgery. *Plast. Reconstr. Surg.* 2014; 134:760–769. [PubMed: 25357035]
11. Cai K, Dong H, Chen C, Yang L, Jandt KD, Deng L. Inkjet printing of laminin gradient to investigate endothelial cellular alignment. *Colloids Surf. B. Biointerfaces.* 2009; 72:230–235. [PubMed: 19419847]
12. Catelas I, Sese N, Wu BM, Dunn JCY, Helgerson S, Tawil B. Human mesenchymal stem cell proliferation and osteogenic differentiation in fibrin gels in vitro. *Tissue Eng.* 2006; 12:2385–2396. [PubMed: 16968177]
13. Chiu YC, Cheng MH, Engel H, Kao SW, Larson JC, Gupta S, Brey EM. The role of pore size on vascularization and tissue remodeling in PEG hydrogels. *Biomaterials.* 2011; 32:6045–6051. [PubMed: 21663958]
14. Cui X, Breitenkamp K, Finn MG, Lotz M, D’Lima DD. Direct Human Cartilage Repair Using Three-Dimensional Bioprinting Technology. *Tissue Eng. Part A.* 2012; 18:1304–1312. [PubMed: 22394017]
15. D’Urso PS, Atkinson RL, Lanigan MW, Earwaker WJ, Bruce IJ, Holmes A, Barker TM, Effeny DJ, Thompson RG. Stereolithographic (SL) biomodelling in craniofacial surgery. *Br. J. Plast. Surg.* 1998; 51:522–530. [PubMed: 9924405]
16. Dorafshar AH, Bojovic B, Christy MR, Borsuk DE, Iloff NT, Brown EN, Shaffer CK, Kelley TN, Kukuruga DL, Barth RN, Bartlett ST, Rodriguez ED. Total face, double jaw, and tongue transplantation: an evolutionary concept. *Plast. Reconstr. Surg.* 2013; 131:241–251. [PubMed: 23076416]
17. Dunham S. *Surgeon’s Helper: 3D Printing Is Revolutionizing Health Care (Op-Ed).* 2015
18. Eshraghi S, Das S. Mechanical and microstructural properties of polycaprolactone scaffolds with one-dimensional, two-dimensional, and three-dimensional orthogonally oriented porous architectures produced by selective laser sintering. *Acta Biomater.* 2010; 6:2467–2476. [PubMed: 20144914]
19. Eshraghi S, Das S. Mechanical and microstructural properties of polycaprolactone scaffolds oriented porous architectures produced by selective laser sintering. *Acta Biomater.* 2010; 6:2467–2476. [PubMed: 20144914]
20. Farias TP, Dias FL, Sousa BA, Galvão MS, Bispo D, Pastl AC. Prototyping: Major Advance in Surgical Planning and Customizing Prostheses in Patients with Bone Tumors of the Head and Neck. *Int. J. Clin. Med.* 2013; 04:1–7.
21. Fernandes da Silva AL, Borba AM, Simão NR, Pedro FLM, Borges AH, Miloro M. Customized polymethyl methacrylate implants for the reconstruction of craniofacial osseous defects. *Case Rep. Surg.* 2014; 2014:358569. [PubMed: 25093139]

22. Fisher M, Dorafshar A, Bojovic B, Manson PN, Rodriguez ED. The Evolution of Critical Concepts in Aesthetic Craniofacial Microsurgical Reconstruction. *Plast. Reconstr. Surg.* 2012;1.
23. Fu Q, Saiz E, Tomsia AP. Direct Ink Writing of Highly Poursous and Strong Glass Scaffolds for Load-bearing Bone Defects Repair and Regeneration. *Acta Biomater.* 2011; 7:3547–3554. [PubMed: 21745606]
24. Gao G, Cui X. Three-dimensional bioprinting in tissue engineering and regenerative medicine. *Biotechnol. Lett.* 2015:1–9.
25. Gao G, Schilling AF, Hubbell K, Yonezawa T, Truong D, Hong Y, Dai G, Cui X. Improved properties of bone and cartilage tissue from 3D inkjet-bioprinted human mesenchymal stem cells by simultaneous deposition and photocrosslinking in PEG-GelMA. *Biotechnol. Lett.* 2015; 37:2349–2355. [PubMed: 26198849]
26. Gao G, Schilling AF, Yonezawa T, Wang J, Dai G, Cui X. Bioactive nanoparticles stimulate bone tissue formation in bioprinted three-dimensional scaffold and human mesenchymal stem cells. *Biotechnol. J.* 2014; 9:1304–1311. [PubMed: 25130390]
27. Van Gestel NAP, Geurts J, Hulsen DJW, Van Rietbergen B, Hofmann S, Arts JJ. Clinical Applications of S53P4 Bioactive Glass in Bone Healing and Osteomyelitic Treatment: A Literature Review. *Biomed Res. Int.* 2015 2015.
28. Gibson I, Rosen DW, Stucker B. Additive Manufacturing Technologies. *Additive Manufacturing Technologies.* 2010:17.
29. Gougoutas AJ, Bastidas N, Bartlett SP, Jackson O. The use of computer-aided design/manufacturing (CAD/CAM) technology to aid in the reconstruction of congenitally deficient pediatric mandibles: A case series. *Int. J. Pediatr. Otorhinolaryngol.* 2015; 79:2332–2342. [PubMed: 26574173]
30. Graham S, Leonidou A, Lester M, Heliotis M, Mantalaris A, Tsiridis E. Investigating the role of PDGF as a potential drug therapy in bone formation and fracture healing. *Expert Opin Investig Drugs.* 2009; 18:1633–1654.
31. He Y, Xue G, Fu J. Fabrication of low cost soft tissue prostheses with the desktop 3D printer. *Sci. Rep.* 2014:4.
32. Hollister SJ, Lin CY, Saito E, Schek RD, Taboas JM, Williams JM, Partee B, Flanagan CL, Diggs A, Wilke EN, Van Lenthe GH, Müller R, Wirtz T, Das S, Feinberg SE, Krebsbach PH. Engineering craniofacial scaffolds. *Orthod. Craniofac. Res.* 2005; 8:162–173. [PubMed: 16022718]
33. Huang TS, Rahaman MN, Doiphode ND, Leu MC, Bal BS, Day DE, Liu X. Freeze extrusion fabrication of 13–93 bioactive glass scaffolds for repair and regeneration of load-bearing bones. *Ceram. Trans.* 2011; 228:45–55.
34. Hung BP, Hutton DL, Kozielski KL, Bishop CJ, Naved B, Green JJ, Caplan AI, Gimble JM, Dorafshar AH, Grayson WL. Platelet-derived growth factor BB enhances osteogenesis of adipose-derived but not bone marrow-derived mesenchymal stromal/stem cells. *Stem Cells.* 2015
35. Hung BP, Naved BA, Nyberg EL, Dias M, Holmes CA, Elisseeff JH, Dorafshar AH, Grayson WL. Three-dimensional printing of bone extracellular matrix for craniofacial regeneration. *ACS Biomater. Sci. Eng.* 2016 acsbomaterials.6b00101.
36. Huttmacher DW, Schantz JT, Lam CXF, Tan KC, Lim TC. State of the art and future directions of scaffold-based bone engineering from a biomaterials perspective. *J. Tissue Eng. Regen. Med.* 2007; 1:245–260. [PubMed: 18038415]
37. Huttmacher DW, Schantz T, Zein I, Ng KW, Teoh SH, Tan KC. Mechanical properties and cell cultural response of polycaprolactone scaffolds designed and fabricated via fused deposition modeling. *J. Biomed. Mater. Res.* 2001; 55:203–216. [PubMed: 11255172]
38. Inzana JA, Olvera D, Fuller SM, Kelly JP, Graeve OA, Schwarz EM, Kates SL, Awad HA. 3D printing of composite calcium phosphate and collagen scaffolds for bone regeneration. *Biomaterials.* 2014; 35:4026–4034. [PubMed: 24529628]
39. Jalbert F, Boetto S, Nadon F, Lauwers F, Schmidt E, Lopez R. One-step primary reconstruction for complex craniofacial resection with PEEK custom-made implants. *J. Cranio-Maxillofacial Surg.* 2014; 42:141–148.
40. Kang H-W, Lee SJ, Ko IK, Kengla C, Yoo JJ, Atala A. A 3D bioprinting system to produce human-scale tissue constructs with structural integrity. *Nat Biotech.* 2016; 34:312–319.

41. Keriquel V, Guillemot F, Arnault I, Guillotin B, Miraux S, Amédée J, Fricain J-C, Catros S. In vivo bioprinting for computer- and robotic-assisted medical intervention: preliminary study in mice. *Biofabrication*. 2010; 2:014101. [PubMed: 20811116]
42. Kim RY, Fasi AC, Feinberg SE. Soft tissue engineering in craniomaxillofacial surgery. 2014
43. Kolan KCR, Leu MC, Hilmas GE, Brown RF, Velez M. Fabrication of 13–93 bioactive glass scaffolds for bone tissue engineering using indirect selective laser sintering. *Biofabrication*. 2011; 3:025004. [PubMed: 21636879]
44. Kolesky DB, Truby RL, Gladman AS, Busbee TA, Homan KA, Lewis JA. 3D bioprinting of vascularized, heterogeneous cell-laden tissue constructs. *Adv. Mater.* 2014; 26:3124–3130. [PubMed: 24550124]
45. Levine JP, Patel A, Saadeh PB, Hirsch DL. Computer-Aided Design and Manufacturing in Craniomaxillofacial Surgery. *J. Craniofac. Surg.* 2012; 23:288–293. [PubMed: 22337427]
46. Loh QL, Choong C. Three-dimensional scaffolds for tissue engineering applications: role of porosity and pore size. *Tissue Eng. Part B. Rev.* 2013; 19:485–502. [PubMed: 23672709]
47. Lohfeld S, Cahill S, Barron V, McHugh P, Dürselen L, Kreja L, Bausewein C, Ignatius A. Fabrication, mechanical and in vivo performance of polycaprolactone/tricalcium phosphate composite scaffolds. *Acta Biomater.* 2012; 8:3446–3456. [PubMed: 22652444]
48. Di Luca A, Ostrowska B, Lorenzo-Moldero I, Lepedda A, Swieszkowski W, Van Blitterswijk C, Moroni L. Gradients in pore size enhance the osteogenic differentiation of human mesenchymal stromal cells in three-dimensional scaffolds. *Sci. Rep.* 2016; 6:22898. [PubMed: 26961859]
49. Di Luca A, Szlazak K, Lorenzo-Moldero I, Ghebes CA, Lepedda A, Swieszkowski W, Van Blitterswijk C, Moroni L. Influencing chondrogenic differentiation of human mesenchymal stromal cells in scaffolds displaying a structural gradient in pore size. *Acta Biomater.* 2016
50. Mandrycky C, Wang Z, Kim K, Kim D-H. 3D bioprinting for engineering complex tissues. *Biotechnol. Adv.* 2015:1–13.
51. McKinstry, RE. Fundamentals of facial prosthetics. ABI Professional publications; 1995.
52. Melchels FPW, Barradas AMC, Van Blitterswijk CA, De Boer J, Feijen J, Grijpma DW. Effects of the architecture of tissue engineering scaffolds on cell seeding and culturing. *Acta Biomater.* 2010; 6:4208–4217. [PubMed: 20561602]
53. Merceron TK, Burt M, Seol Y-J, Kang H-W, Lee SJ, Yoo JJ, Atala A. A 3D bioprinted complex structure for engineering the muscle–tendon unit. *Biofabrication*. 2015; 7:035003. [PubMed: 26081669]
54. Murphy CM, Haugh MG, O'Brien FJ. The effect of mean pore size on cell attachment, proliferation and migration in collagen–glycosaminoglycan scaffolds for bone tissue engineering. *Biomaterials*. 2010; 31:461–466. [PubMed: 19819008]
55. Navarro M, Michiardi a, Castaño O, Planell Ja. Biomaterials in orthopaedics. *J. R. Soc. Interface*. 2008; 5:1137–1158. [PubMed: 18667387]
56. Obregon F, Vaquette C, Ivanovski S, Hutmacher DW, Bertassoni LE. Three-Dimensional Bioprinting for Regenerative Dentistry and Craniofacial Tissue Engineering. 2015; XX:1–10.
57. Parthasarathy J. 3D modeling, custom implants and its future perspectives in craniofacial surgery. *Ann. Maxillofac. Surg.* 2014; 4:9. [PubMed: 24987592]
58. Pati F, Song T-H, Rijal G, Jang J, Kim SW, Cho D-W. Ornamenting 3D printed scaffolds with cell-laid extracellular matrix for bone tissue regeneration. *Biomaterials*. 2015; 37:230–241. [PubMed: 25453953]
59. Peled M, El-Naaj IA, Lipin Y, Ardekian L. The use of free fibular flap for functional mandibular reconstruction. *J. Oral Maxillofac. Surg.* 2005; 63:220–224. [PubMed: 15690291]
60. Perez RA, Mestres G. Role of pore size and morphology in musculo-skeletal tissue regeneration. *Mater. Sci. Eng. C Mater. Biol. Appl.* 2016; 61:922–939. [PubMed: 26838923]
61. Podolsky DJ, Mainprize JG, Edwards GP, Antonyshyn OM. Patient-Specific Orbital Implants: Development and Implementation of Technology for More Accurate Orbital Reconstruction. *J. Craniofac. Surg.* 2016; 27:131–133. [PubMed: 26674886]
62. Rasperini G, Pilipchuk SP, Flanagan CL, Park CH, Pagni G, Hollister SJ, Giannobile WV. 3D-printed bioresorbable scaffold for periodontal repair. *J. Dent. Res.* 2015; 94:153S–157S. [PubMed: 26124215]

63. Rodby KA, Turin S, Jacobs RJ, Cruz JF, Hassid VJ, Kolokythas A, Antony AK. Advances in oncologic head and neck reconstruction: Systematic review and future considerations of virtual surgical planning and computer aided design/computer aided modeling. *J. Plast. Reconstr. Aesthetic Surg.* 2014; 67:1171–1185.
64. Roohani-Esfahani S-I, Newman P, Zreiqat H. Design and Fabrication of 3D printed Scaffolds with a Mechanical Strength Comparable to Cortical Bone to Repair Large Bone Defects. *Sci. Rep.* 2016; 6:19468. [PubMed: 26782020]
65. Sawyer AA, Song SJ, Susanto E, Chuan P, Lam CXF, Woodruff MA, Huttmacher DW, Cool SM. The stimulation of healing within a rat calvarial defect by mPCL–TCP/collagen scaffolds loaded with rhBMP-2. *Biomaterials.* 2009; 30:2479–2488. [PubMed: 19162318]
66. Seruya M, Borsuk DE, Khalifian S, Carson BS, Dalesio NM, Dorafshar AH. Computer-aided design and manufacturing in craniocynostosis surgery. *J. Craniofac. Surg.* 2013; 24:1100–1105. [PubMed: 23851748]
67. Shan X-F, Chen H-M, Liang J, Huang J-W, Cai Z-G. Surgical Reconstruction of Maxillary and Mandibular Defects Using a Printed Titanium Mesh. *J. Oral Maxillofac. Surg.* 2015; 73:1437.e1–1437.e9. [PubMed: 25971919]
68. Suwanprateeb J, Sannang R, Suvannapruk W, Panyathanmaporn T. Mechanical and in vitro performance of apatite–wollastonite glass ceramic reinforced hydroxyapatite composite fabricated by 3D-printing. *J. Mater. Sci. Mater. Med.* 2009; 20:1281–1289. [PubMed: 19225870]
69. Tanner PB, Mobley SR. External auricular and facial prosthetics: a collaborative effort of the reconstructive surgeon and anaplastologist. *Facial Plast. Surg. Clin. North Am.* 2006; 14:137–145. [PubMed: 16750771]
70. Temple JP, Hutton DL, Hung BP, Huri PY, Cook CA, Kondragunta R, Jia X, Grayson WL. Engineering anatomically shaped vascularized bone grafts with hASCs and 3D-printed PCL scaffolds. *J. Biomed. Mater. Res. A.* 2014; 102:4317–4325. [PubMed: 24510413]
71. Thomas KF. *The art of clinical anaplastology.* 2006
72. Visser A, Raghoobar GM, van Oort RP, Vissink A. Fate of implant-retained craniofacial prostheses: life span and aftercare. *Int. J. Oral Maxillofac. Implants.* 2007; 23:89–98.
73. Wang S, Wong Po Foo C, Warriar A, Poo M-M, Heilshorn SC, Zhang X. Gradient lithography of engineered proteins to fabricate 2D and 3D cell culture microenvironments. *Biomed. Microdevices.* 2009; 11:1127–1134. [PubMed: 19495986]
74. Wilkins LM, Watson SR, Prosky SJ, Meunier SF, Parenteau NL. Development of a bilayered living skin construct for clinical applications. *Biotechnol. Bioeng.* 1994; 43:747–756. [PubMed: 18615798]
75. Yanez M, Rincon J, Dones A, De Maria C, Gonzales R, Boland T. In Vivo Assessment of Printed Microvasculature in a Bilayer Skin Graft to Treat Full-Thickness Wounds. *Tissue Eng. Part A.* 2014; 00:1–10.
76. Yuan H, Fernandes H, Habibovic P, de Boer J, Barradas AMC, de Ruiter A, Walsh WR, van Blitterswijk CA, de Bruijn JD. Osteoinductive ceramics as a synthetic alternative to autologous bone grafting. *Proc. Natl. Acad. Sci. U. S. A.* 2010; 107:13614–13619. [PubMed: 20643969]
77. Zhang Y, Yin C, Zheng C, Zhou K. Computational hydrographic printing. *ACM Trans. Graph.* 2015; 34:131:1–131:11.
78. Zhou Y, Huttmacher DW, Varawan S, Lim TM. In vitro bone engineering based on polycaprolactone and polycaprolactone – tricalcium phosphate composites. *Polym. Int.* 2007; 342:333–342.
79. Zuo KJ, Wilkes GH. Clinical Outcomes of Osseointegrated Prosthetic Auricular Reconstruction in Patients With a Compromised Ipsilateral Temporoparietal Fascial Flap. *J. Craniofac. Surg.* 2016; 27:44–50. [PubMed: 26703031]
80. Struct3Dat <<http://www.estructur3d.io/>>
81. Lazarus3Dat <<http://www.laz3d.com/>>
82. Picsimaat <<http://www.picsima.com/>>
83. e-Nableat <<http://enablingthefuture.org/>>
84. Osteoporeat <<http://www.osteopore.com.sg/index.html>>

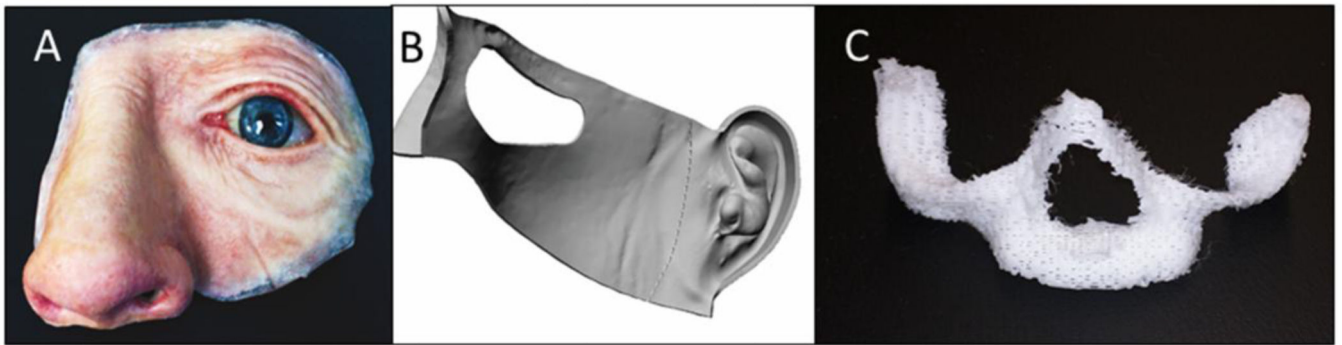


Figure 1. Examples of Rehabilitation, Reconstruction, and Regeneration. (A) Custom PDMS midfacial and ocular prosthesis. (B) Cutting and placement guides for auricular autogenous reconstruction. (C) 3D-printed maxilla, porous PCL scaffold.



Figure 2.

(A) Orbital mold 3D model obtained through a fully digital workflow. (B, C) Resulting 3D-printed 3-piece mold that can be used for casting PDMS prosthesis. (D) The final PDMS prosthesis can be colored and provide satisfactory cosmesis. Photos used with author's permission. (Perry, R. The Development of an Orbital Prosthesis Workflow Using Advanced Digital Technologies, A thesis submitted to Johns Hopkins University in conformity with the requirements for the degree of Master of Arts, Baltimore, Maryland October, 2015)

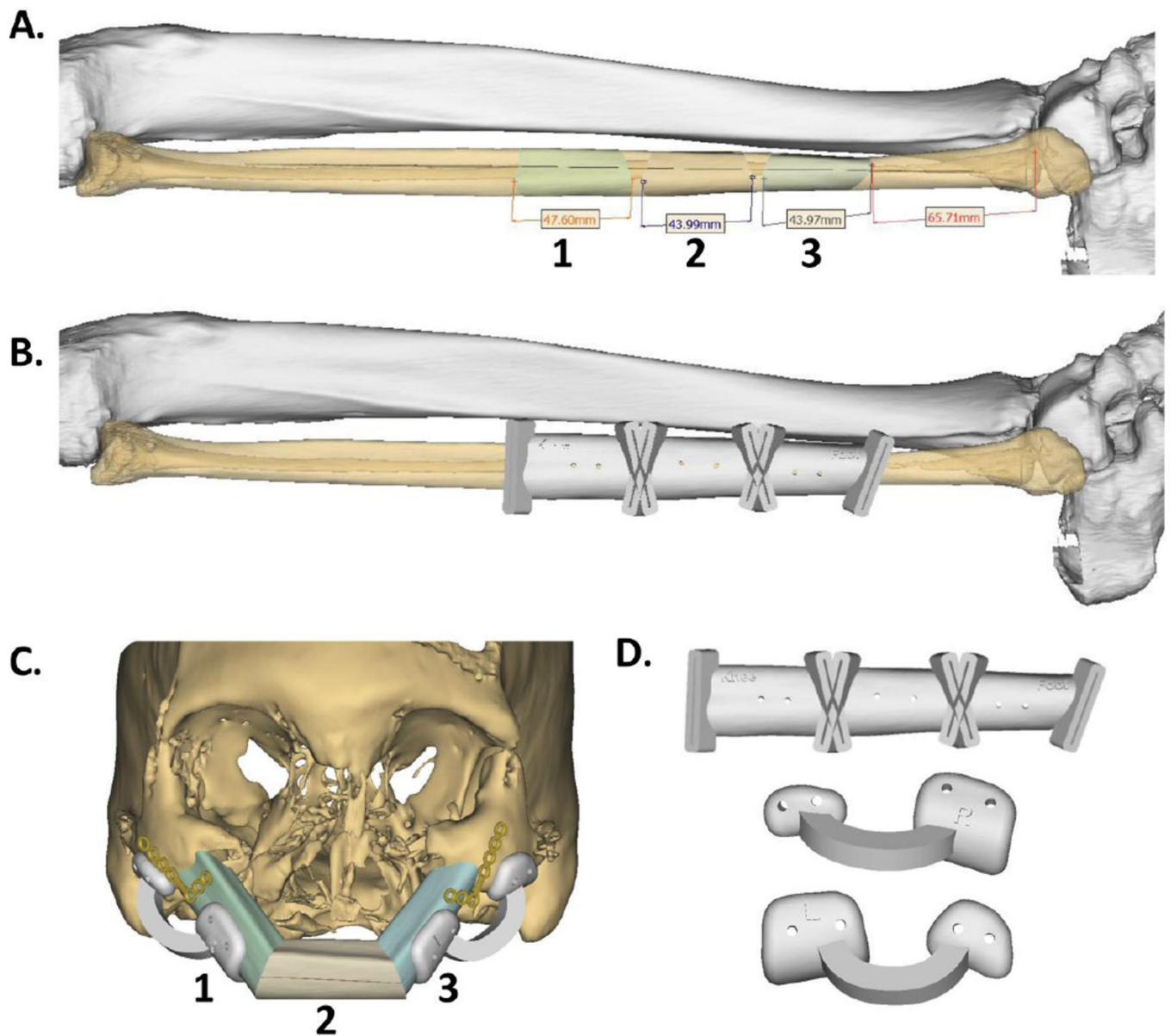


Figure 3. Synthes Pro Plan Virtual Surgery Plan and 3D-printing Cutting and Placement Guides. (A) Pre-operative CT Scan of the right fibula. Graft pieces are labeled beginning 6.6 cm from the distal end of the fibula. (B) Planned cutting guide superimposed over the fibula. (C) Planned fibular flaps in the context of the remaining zygoma, using the positioning guides and exact graft pieces. (D) 3D-printed parts delivered to the surgeon include an anatomic guide, the fibula cutting guide, and positioning guides.

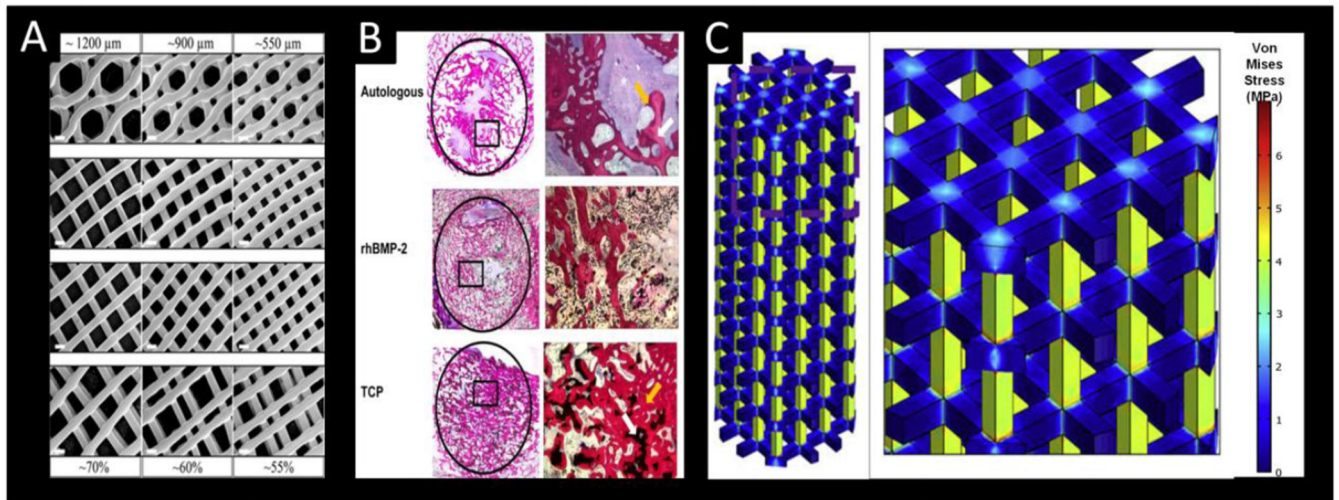


Figure 4.

3D-printed scaffolds. (A) The scaffold should have appropriate micro-architecture, encompassing pore size and porosity. Using direct ink writing of a ceramic powder in a viscoelastic solution, different well-defined pore geometries were manufactured and visualized under scanning electron microscopy. Scale bars represent 500 μm . Adapted from⁶⁴. (B) Cells residing within the scaffold should be signaled appropriately to regenerate tissue. Sintered tricalcium phosphate scaffolds were implanted in critically sized iliac defects in sheep. Bone formation by resident cells, denoted by the red stain, is evident when compared against other osteoinductive materials (bone morphogenetic protein and autologous bone graft). Adapted from⁷⁶. (C) The mechanical properties of the scaffold must be appropriate for the tissue being regenerated. Selective laser sintering of polycaprolactone was used to fabricate a porous cylinder, which was tested mechanically to result in a stiffness of 15 MPa, within the range of trabecular bone. Adapted from¹⁹.

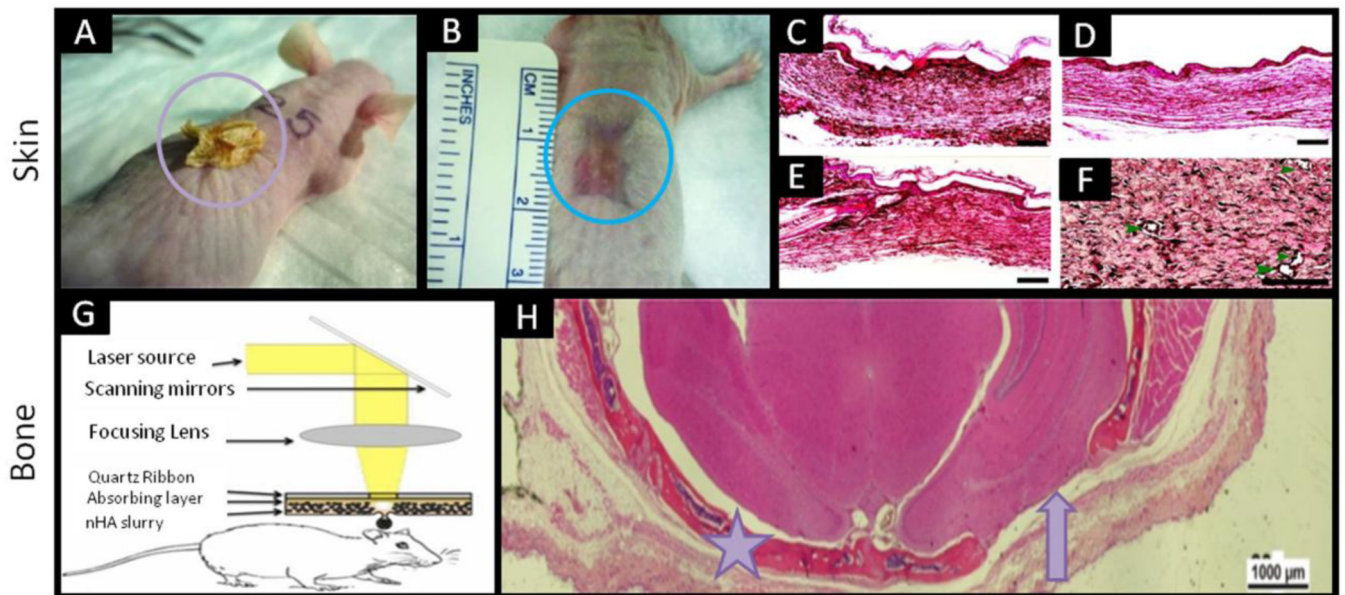


Figure 5.

Bioprinting for engineering skin and bone tissues. Full thickness dermal wounds after 4 weeks of healing with (A) Apligraf applied, denoted by the yellow circle and (B) 3D-bioprinted skin applied denoted by the blue circle. Severe wound contraction and scaffold drying took place in the Apligraf scaffold compared to the bioprinted scaffold with microvessels. C–E. H&E stains of (C) Apligraf, (D) no treatment, and (E) 3D-bioprinted skin scaffold. (F) A higher magnification image of 2 weeks of healing following application of 3D bioprinted skin. Adapted from⁷⁵. (G) Schematic of laser-assisted bioprinting directly into mouse calvarial defect. nHA slurry refers to a nano-hydroxyapatite suspended in a glycerol solution for printing. (H) H&E stain 3 months after calvarial defects were made. Bone healing observed in the area where the 3D bioprinted scaffold was applied (denoted by the star) and no bone healing in the no scaffold control (denoted by the arrow). G and H adapted from⁴¹.

Table 1

Summary of 3D-printing technologies used for treating craniofacial deformities

Treatment Type	3D Printing Applications	Printing Methods	Materials	Qualities of
Prosthetic Rehabilitation (Improve patient aesthetics)	<input type="checkbox"/> Molds for casting duplicates <input type="checkbox"/> Printed prostheses <input type="checkbox"/> Surgical guides <input type="checkbox"/> Auricle, orbit, and nose rehabilitation	<input type="checkbox"/> Inkjet <input type="checkbox"/> FDM	PDMS ABS PMMA	The material should non-degradable, anatomic shape or create a rigid to case PDMS
Reconstruction (Tissue grafting)	<input type="checkbox"/> Surgical positioning and cutting guides <input type="checkbox"/> Custom metal implants <input type="checkbox"/> Bone reconstruction	<input type="checkbox"/> FDM, <input type="checkbox"/> Stereolithography <input type="checkbox"/> Laser sintering <input type="checkbox"/> Direct-ink writing	Titanium PEEK Polypropylene Bioglasses PLA ABS PMMA Hydroxyapatite	The material should degradable, and that the surgeon graft into place.
Tissue Regeneration (Recapitulate native tissue structure and function)	<input type="checkbox"/> Scaffold generation <input type="checkbox"/> Cellular constructs <input type="checkbox"/> Bone, cartilage, skin, muscle <input type="checkbox"/> Composite craniofacial tissues	Acellular: <input type="checkbox"/> SLS <input type="checkbox"/> FDM	PCL Calcium Phosphate	The material should and porous. Bioactivity, properties, and should mimic healthy
		Bioprinting: <input type="checkbox"/> Inkjet <input type="checkbox"/> Extrusion <input type="checkbox"/> Laser-assisted <input type="checkbox"/> Stereolithography	Fibrinogen Gelatin Alginate	The material should Bioactivity and of the native tissue mimicked.

Author Manuscript

Author Manuscript

Author Manuscript

Author Manuscript